Microscopic Mechanism for a Higher-Spin Kitaev Model

P. Peter Stavropoulos,[1] D. Pereira,[1] and Hae-Young Kee[1,2,*]
[1]Department of Physics and Center for Quantum Materials, University of Toronto, 60 St. George St., Toronto, Ontario, M5S 1A7, Canada
[2]Canadian Institute for Advanced Research, Toronto, Ontario, M5G 1Z8, Canada

(Received 26 February 2019; published 19 July 2019)

The spin $S = \frac{1}{2}$ Kitaev honeycomb model has attracted significant attention since emerging candidate materials have provided a playground to test non-Abelian anyons. The Kitaev model with higher spins has also been theoretically studied, as it may offer another path to a quantum spin liquid. However, a microscopic route to achieve higher spin Kitaev models in solid state materials has not been rigorously derived. Here we present a theory of the spin $S = 1$ Kitaev interaction in two-dimensional edge-shared octahedral systems. Essential ingredients are strong spin-orbit coupling in anions and strong Hund's coupling in transition metal cations. The $S = 1$ Kitaev and ferromagnetic Heisenberg interactions are generated from superexchange paths. Taking into account the antiferromagnetic Heisenberg term from direct-exchange paths, the Kitaev interaction dominates the physics of the $S = 1$ system. Using an exact diagonalization technique, we show a finite regime of $S = 1$ spin liquid in the presence of the Heisenberg interaction. Candidate materials are proposed, and generalization to higher spins is discussed.

DOI: 10.1103/PhysRevLett.123.037203

Introduction.—Highly entangled quantum spin liquids provide exotic phenomena including fractional excitations [1,2]. Among several proposed quantum spin liquid models, an exactly solvable model is a bond-dependant interaction of spin $S = \frac{1}{2}$ on the two-dimensional (2D) honeycomb lattice proposed by Kitaev [3]. The ground state of the $S = \frac{1}{2}$ Kitaev model offers non-Abelian anyons under a magnetic field. Recently the smoking-gun evidence of such particles was supported by the half-integer quantized thermal Hall conductivity in α-$RuCl_3$ [4], making it the most promising candidate to display Kitaev physics.

Along with the rapid progress on the $S = \frac{1}{2}$ Kitaev spin liquids in solid state materials [5–24], the theoretical condensed matter physics community has considered a higher spin S Kitaev model. A first attempt was made by Baskaran and collaborators [25]. They showed that for arbitrary spin S, localized Z_2 flux excitations are present, as plaquette operators can be constructed, and a vanishing spin-spin correlation beyond nearest neighbors is found [26]. Unlike the $S = \frac{1}{2}$ model, the higher S Kitaev model is not exactly solvable, and several numerical studies have been performed. In particular, the $S = 1$ Kitaev model has been studied by using exact diagonalization (ED) and thermal pure quantum (TPQ) techniques and it was suggested that the ground state of the $S = 1$ Kitaev model may be a gapless spin liquid [27]. Using high-temperature series expansions and TPQ, a double peak structure in the specific heat similar to $S = \frac{1}{2}$ and an incipient entropy plateau at value of $\frac{1}{2}\ln 3$ were found in the $S = 1$ model [27,28]. Dynamics of the classical ($S \to \infty$) Kitaev spin liquid was also studied and it was suggested that the quantum model can be understood by fractionalization of magnons in one-dimensional manifolds [29]. While these theoretical results promote another path to quantum spin liquids, there has been a lack of microscopic routes to achieve spin S Kitaev model in solid state materials.

In this Letter, we present a way to generate the $S = 1$ bond-dependent Kitaev interaction in 2D Mott insulators with edge-shared octahedra. Two essential ingredients are strong Hund's coupling among two electrons in e_g orbitals and strong spin-orbit coupling (SOC) at anion sites. Using a strong coupling expansion, we show that the bond-dependant interactions are generated via superexchange between two cations with e_g orbitals mediated by anion p orbital electrons with strong SOC. 12- and 18-site ED results of the $S = 1$ Kitaev-Heisenberg (KH) model show a finite regime of the Kitaev spin liquid. Candidate materials are proposed, and generalization to higher spin bond-dependent interactions are also discussed.

Microscopic mechanism for the $S = 1$ Kitaev model.—We consider a 2D edge-shared octahedral system with two types of atoms. The honeycomb (or triangular) network is made of transition metal (M) cations with half filled e_g orbitals such as d^8 electronic configuration. The anion (A) atoms with fully occupied p orbitals form edge-shared octahedral cages around every M site as shown in Fig. 1. The Hamiltonian consists of the on-site interactions H_0 and hopping between the M and A sites, H_{kin}. For $3d$ transition metals, such as Ni^{2+}, typical energy scales of the hopping parameters are smaller than the energy scales of the on-site H_0, which allows the use of standard strong coupling

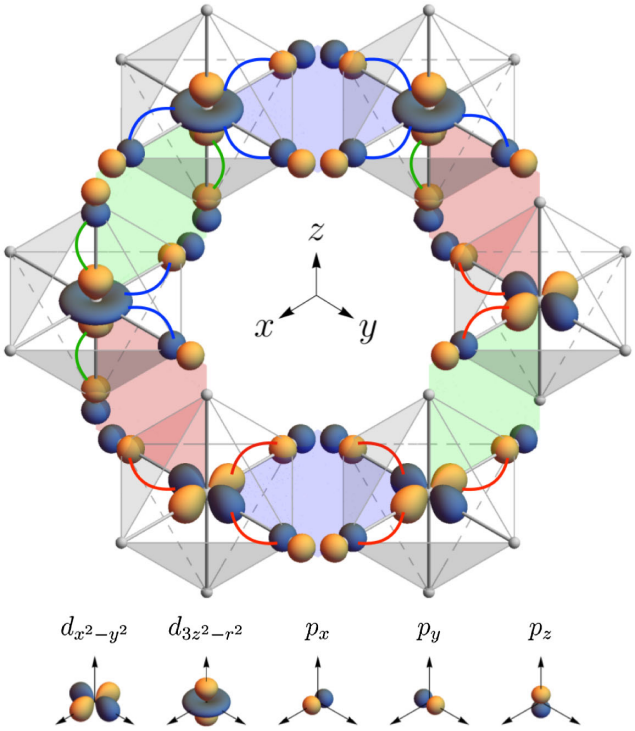

FIG. 1. Indirect hopping integrals between M and A sites are denoted by the colored curved lines. The red, green, and blue colors represent t_1, t_2, and t_3, respectively, and the sign of the hopping integrals is ignored for simplicity. The M sites with e_g orbitals are located in the center of each octahedral cage formed by A sites occupied by three p orbitals. The Kitaev bond-dependent interactions X, Y, and Z bonds are, respectively, represented by the red, green, and blue shaded regions. For clarity, every A site is drawn by two separated A sites to represent different hopping contributions from different p and e_g orbitals. The global coordinates of the x, y, and z axes are shown in the center of the honeycomb plane.

expansion theory. The on-site Hamiltonian of both M and A sites is described by the Kanamori interaction [30] and SOC:

$$H_0 = U\sum_{\alpha} n_{\alpha\uparrow}n_{\alpha\downarrow} + \frac{U'}{2}\sum_{\substack{\alpha\neq\beta,\\ \sigma,\sigma'}} n_{\alpha\sigma}n_{\beta\sigma'} + \lambda \mathbf{l}\cdot\mathbf{s} - \frac{J_H}{2}\sum_{\substack{\alpha\neq\beta,\\ \sigma,\sigma'}} c^{\dagger}_{\alpha\sigma}c^{\dagger}_{\beta\sigma'}c_{\beta\sigma}c_{\alpha\sigma'} + J_H\sum_{\alpha\neq\beta} c^{\dagger}_{\alpha\uparrow}c^{\dagger}_{\alpha\downarrow}c_{\beta\downarrow}c_{\beta\uparrow}, \quad (1)$$

where the density operator $n_{\alpha\sigma}$ is given by $c^{\dagger}_{\alpha\sigma}c_{\alpha\sigma}$, and $c^{\dagger}_{\alpha\sigma}$ is the creation operator with α orbital and spin σ. U and U' are the intraorbital and interorbital density-density interaction, respectively, and J_H is the Hund's coupling for the spin-exchange and pair-hopping terms. Operators $\mathbf{l}$ and $\mathbf{s}$, respectively, denote angular momentum and spin for orbital α and spin σ, and λ denotes the strength of SOC.

In general, the competition between Hund's coupling and SOC leads to a different atomic state [31]. For the M sites with e_g orbitals, the SOC is inactive when the crystal field splitting between t_{2g} and e_g is bigger than the SOC strength. Here we consider d^8 systems, such as Ni^{2+}, where t_{2g} orbitals are fully filled, and the crystal field splitting is larger than the SOC. In this case, the SOC does not mix the e_g states, as the e_g orbitals are made of the z component of angular momentum of ± 2 and 0. In the half-filed e_g orbitals the Hund's coupling selects the total spin $S = 1$ state with energy $U' - J_H$. On the other hand, for the A sites with p orbitals, the SOC splits the p orbitals into total angular momentum $j = \frac{3}{2}$ and $j = \frac{1}{2}$ states. The Hund's coupling for A sites is only relevant for excited states in the perturbation theory. The full energy spectrum of H_0 required for the perturbation theory is listed in Table 1 in the Supplemental Material [32]. To differentiate U, U', J_H for the d and p orbitals, we use the subscript d/p for $U_{d/p}$, $U'_{d/p}$, and $J_{H_{d/p}}$, which refer to the on-site interactions for d/p orbitals from now on. Similarly, we use $d^{\dagger}$ and $p^{\dagger}$ to represent creation operators for the d and p orbital, respectively. For SOC, we have only λ_p because λ_d is inactive in the e_g orbitals when the crystal field splitting is larger than the SOC, which is the case for $3d$ systems.

Let us consider the nearest neighbor (NN) hopping parameters between the M and A sites to construct a minimal NN spin model. Since the p orbitals are fully filled, and e_g orbitals are half filled, we consider holes rather than electrons. Then in the ground state of the atomic Hamiltonian H_0, there is no hole in the p orbitals while e_g orbitals are half filled. It is straightforward to build the tight-binding model:

$$H_{\mathrm{kin}} = \sum_{\substack{\langle i,j\rangle\\ \sigma}} d^{\dagger}_{i,\alpha\sigma}M^{(i,j)}_{\alpha,\beta}p_{j,\beta\sigma} + \mathrm{H.c.}, \quad (2)$$

where $d^{\dagger}_{i,\alpha\sigma}(p^{\dagger}_{j,\beta\sigma})$ creates one of the $d(p)$ orbitals denoted by $\alpha(\beta)$ and spin σ on site $i(j)$. The hopping matrix $M^{(i,j)}$ depends on the (i,j) bond. As shown in Fig. 1, there are three distinct hopping integrals t_1, t_2, and t_3 denoted by the red, blue, and green colored curves, respectively. They appear on different bonds. For example,

$$\begin{aligned}
&\text{along the } x \text{ axis}: \; t_1 d^{\dagger}_{i,x^2-y^2}p_{j,x} - t_2 d^{\dagger}_{i,3z^2-r^2}p_{j,x} + \mathrm{H.c.},\\
&\text{along the } y \text{ axis}: \; -t_1 d^{\dagger}_{i,x^2-y^2}p_{j,y} - t_2 d^{\dagger}_{i,3z^2-r^2}p_{j,y} + \mathrm{H.c.},\\
&\text{along the } z \text{ axis}: \; t_3 d^{\dagger}_{i,3z^2-r^2}p_{j,z} + \mathrm{H.c.}
\end{aligned} \quad (3)$$

All other bond directions are related by symmetry such as mirror symmetry, and the set of tight binding parameters is given in Table 2 in the Supplemental Material [32]. They can be represented by the Slater-Koster parameters [33], i.e., $t_1 = (\sqrt{3}/2)t_{pd\sigma}$, $t_2 = \frac{1}{2}t_{pd\sigma}$, $t_3 = t_{pd\sigma}$ if the perfect cubic symmetry is preserved.

Treating the tight binding Hamiltonian $H_{\rm kin}$ as a perturbation to the on-site Hamiltonian H_0, a NN spin model for $S=1$ on the honeycomb lattice with edge-shared octahedra via superexchange processes is determined. Before we derive the model explicitly, it is straightforward to check that the symmetry of the edge-shared octahedral crystal allows Heisenberg J, Kitaev K, and symmetric off-diagonal Γ interactions [11,34,35].

There are several processes that contribute to the spin interaction and we categorize them by the number of holes at a given site. The one hole processes include intermediate states with one hole at most on any A site and the two hole processes include intermediate states with two holes on an A site. In the one hole processes, the SOC λ_p generates intermediate states of different energies, depending on whether the one hole state is $j=\frac{1}{2}$ or $\frac{3}{2}$. For the two hole process, p orbital Hund's coupling J_{H_p} becomes as important as the SOC, and we will consider two limits of $J_{H_p}\to 0$ and $\lambda_p\to 0$ to show the origin of the Kitaev interaction.

Taking into account all possible fourth-order superexchange processes shown in the Supplemental Material [32], the resulting NN spin model consists of the Kitaev and Heisenberg interactions:

$$H^{\gamma}_{\langle ij\rangle}=K^{\gamma}S^{\gamma}_i S^{\gamma}_j+J_{\rm ind}\mathbf{S}_i\cdot\mathbf{S}_j, \tag{4}$$

where i, j are NN sites, and γ refers the X-, Y-, and Z-bond type. $\mathbf{S}$ is the spin 1 operator and its bond-dependent interaction takes the $\gamma=x$, y, z spin component. The spin components are directed along the cubic axes of the underlying ligand octahedra, so the honeycomb layer lies in a plane perpendicular to the [111] spin direction as shown in Fig. 1. Note that the Γ term is exactly 0 within the fourth-order term, and $J_{\rm ind}=-\frac{1}{2}K^{\gamma}$.

The expressions of K^{γ} and $J_{\rm ind}$ are presented in the Supplemental Material [32] and they can be simplified in certain limits. With the cubic symmetry, i.e., $t_1^2=\frac{3}{4}t_3^2$ and $t_2^2=\frac{1}{4}t_3^2$, $K^{x/y}=K^z\equiv K$. When U_d and the atomic potential difference Δ between the M (ϵ_M) and A (ϵ_A) sites (i.e., $\Delta\equiv\epsilon_M-\epsilon_A$) are the largest energy scales, it simplifies to

$$K\sim\frac{3}{2}\lambda_p^2 t_{pd\sigma}^4\left(\frac{1}{(2U_d+\Delta)^5}+\frac{1}{2U_d(2U_d+\Delta)^4}\right). \tag{5}$$

For a Mott insulator, i.e., $\Delta>U_d$, one can further simplify to $K\sim\frac{3}{4}(\lambda_p^2 t_{pd\sigma}^4/U_d\Delta^4)\equiv\frac{3}{4}(t_{\rm ind}^2/U_d)$, where $t_{\rm ind}=(\lambda_p t_{pd\sigma}^2/\Delta^2)$ describes the effective hopping between the M and M site via the A sites. When the cubic symmetry is slightly broken, a slight difference between K^z and $K^{x/y}$ appears as shown in the Supplemental Material [32]. The Heisenberg interaction $J_{\rm ind}$ via the superexchange process is ferromagnetic and its strength is half of the K term. Interestingly, $J_{\rm ind}$ is finite when the large SOC of the anion sites is present, even when Hund's coupling J_{H_p} is absent. For the other limit of $\lambda_p\to 0$, the ferromagnetic Heisenberg interaction from two-hole processes is found and the Kitaev term vanishes.

There is also a direct hopping t between the M sites, which leads to the antiferromagnetic Heisenberg term $J_{\rm dir}\sim 4t^2/U_d$. Given the distance between the M and A sites vs M sites, the direct hopping integral t is an order of magnitude smaller than the indirect t_1, t_2, t_3 hoppings; however, the perturbation process involves second order terms. Thus the antiferromagnetic Heisenberg term $J_{\rm dir}$ of similar strength to the ferromagnetic term $J_{\rm ind}$ may be generated via direct hopping. Since the direct and indirect Heisenberg terms come with opposite signs, one may expect a small total Heisenberg interaction $J\equiv J_{\rm dir}-|J_{\rm ind}|$ and the Kitaev interaction dominates the physics of the spin $S=1$ systems.

Exact diagonalization of $S=1$ KH model.—We show that the NN spin model of two electrons in the e_g orbitals surrounded by anions with strong SOC forming edge-shared octahedra consists of the $S=1$ Kitaev and Heisenberg interactions. It is worthwhile to check if the $S=1$ Kitaev spin liquid survives in the presence of the Heisenberg term. We carry out ED calculations to determine the phase diagram near the antiferromagnetic Kitaev term. The ED results are shown in Fig. 2(a) on two clusters of $N=12$ and $N=18$ sites using the periodic boundary conditions in Figs. 2(b) and 2(c), respectively. Phase transitions are identified by the singular behavior of the second derivative of the ground state energy density ($u_{\rm GS}$) with respect to the variable J/K, i.e., $-\partial^2_{J/K}u_{\rm GS}$.

Our results show three phases. A finite region of the Kitaev phase around the antiferromagnetic K point appears with a J/K window of width $\sim$0.06, similar to the spin $\frac{1}{2}$ with a J/K window of $\sim$0.07 [9]. While the Kitaev phase occupies a narrow phase space at zero temperature, it would govern physical properties of finite temperature and finite magnetic fields, similar to the spin $\frac{1}{2}$ systems, if the system can be tuned closer to the Kitaev phase. To clarify the nature of the three phases, we examine the spin-spin (SS) correlations of the three regions using the 12-site cluster, which are shown in Fig. 2 of the Supplemental Material [32]. The SS correlation is finite only on the NN bond, and zero for any further neighbors at $J/K=0$, consistent with the pure Kitaev $S=1$ phase [25]. For $J/K\sim 0.3$ we find antiferromagnetic (AFM) correlations, while for $J/K\sim -0.3$ the zigzag (ZZ) correlations are present. These magnetically ordered phases match the magnetic orderings found in the spin $\frac{1}{2}$ and classical spin model results [9]. The phase transitions seem to be of first order, but due to finite size effects, an intrinsic problem of the ED technique, further studies are required to pin down the nature of the transitions.

Kitaev candiate materials.—A single layer of NiI_2 is a candidate for $S=1$ Kitaev materials on a triangular lattice.

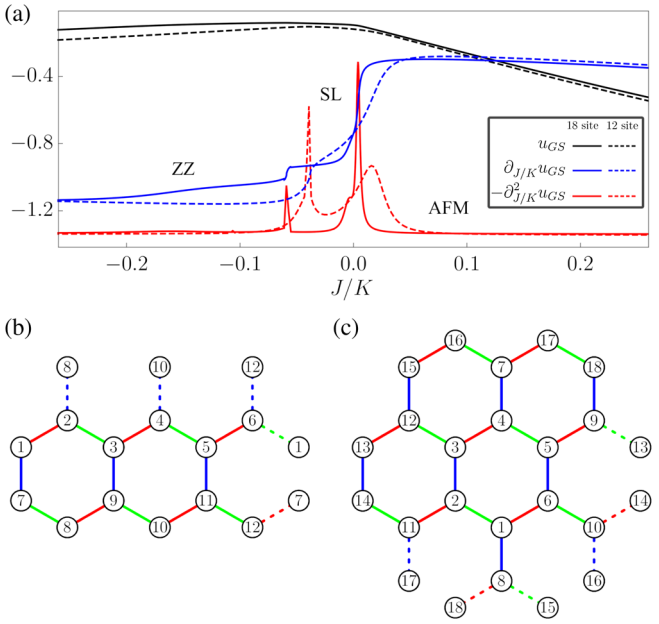

FIG. 2. (a) The phase diagram of the $S = 1$ KH model. By tuning the ratio of J/K, two transitions signaled by the singular behavior of first (blue) and second (red) derivative of the ground state energy density u_{GS} are found on both the 12- and 18-site ED clusters shown in (b) and (c), respectively. Energy density units are $\sqrt{J^2 + K^2}/N$. There are three phases identified by spin-spin correlators as discussed in the main text. The Kitaev spin liquid (SL) appears near $J/K \sim 0$, and AFM and ZZ orderings are, respectively, found in the antiferromagnetic and ferromagnetic Heisenberg interaction regions.

The triangular lattice has X, Y, and Z bond defined similarly to the honeycomb lattice and the above derivation of the mechanism is applicable. The bulk compounds form triangular layers of Ni cations and I anions form edge-shared octahedral cages around Ni. While the bulk $NiCl_2$ is ferromagnetic below 52 K [36], the heavier sister compound NiI_2 has helimagnetic order below 75 K [37,38]. The helical ordering in the bulk compound is related to the layer coupling as the ordering wave vector involves the lattice vector perpendicular to the triangular layer [38]. Thus a single layer of NiI_2 is desirable to test the dominant Kitaev interaction.

Another group of potential materials is the layered transitional metal (M) oxide compounds $A_3Ni_2XO_6$ ($A = \mathrm{Li}$, Na, $X = \mathrm{Bi}$, Sb). Unlike the simple binary NiI_2, the M sites are surrounded by edge-shared oxygen octahedral cages, forming layers of honeycomb networks sandwiched between layers of the alkali A sites. X sites reside in the center of the honeycomb. $A_3Ni_2XO_6$ exhibits ZZ ordering at low temperatures [39,40]. There are 2 electrons in e_g orbitals making total spin $S = 1$ states, a good example for the proposed mechanism. The strong SOC may occur via proximity to the heavy X atoms. While the oxygen has a weak atomic SOC, the heavy X atoms with strong SOC λ_X induce splitting among the p orbitals of the oxygen atoms leading to similar effects presented above. For instance, the effective SOC could be enhanced when one considers hopping between X and O sites denoted by t_{pp}. Using a perturbative approach, the strength of the effective SOC in the p orbitals of O sites is then determined by $\tilde{\lambda}_p \sim \{[t_{pp}^2/\tilde{\Delta} - (\lambda_{\mathrm{X}}/2)] - [t_{pp}^2/\tilde{\Delta} + \lambda_{\mathrm{X}}]\}$, where $\tilde{\Delta}$ is an atomic potential difference between the X and O atoms. While it is difficult to quantify $\tilde{\lambda}_p$ in this case, we note that the specific heat measurements resulting in entropy of $\sim\frac{1}{2}\log 3$ per Ni above the Néel temperature for both $Li_3Ni_2SbO_6$ and $Na_3Ni_2SbO_6$ [39] strongly hint that they are promising candidates for $S = 1$ Kitaev honeycomb materials.

Outlook and summary.—The bond-dependent interactions are ubiquitous in Mott insulators with an edge-shared octahedral environment and strong SOC. This is because SOC mixes different orbitals and spin components at a given site, and bond-dependent spin interactions rely on the hopping integrals of the bond, whose size is determined from the overlap of relevant orbitals. However, the approach taken in the compass [5] and generic spin model [11] does not work for higher spins. This is because Hund's coupling, which maximizes the total spin, is necessary for a higher spin such as $S = 1$ of two electrons in e_g or $S = 3/2$ of three electrons in t_{2g}. On the other hand, the bond-dependent interaction requires a mixture of spins via SOC, which works against the Hund's coupling. Thus it has been unclear how to generate a higher spin Kitaev model.

Here we derive a microscopic $S = 1$ Kitaev interaction via superexchange processes between half-filled e_g orbital cations mediated by p orbital anions with strong SOC using the standard strong coupling expansion. We find the dominant interaction is the antiferromagnetic Kitaev term, whose strength is twice as big as that of the ferromagnetic Heisenberg interaction. Taking into account the direct exchange process that results in an antiferromagnetic Heisenberg term, we expect that the Kitaev interaction dominates spin physics of these Mott insulators. A small region of $S = 1$ Kitaev phase with only NN spin-spin correlation is found in 12- and 18-site ED calculations. A finite ferromagnetic Heisenberg interaction stabilizes the ZZ magnetic ordering nearby the spin liquid. $S = 1$ Kitaev candidates include a single layer of NiI_2 on the triangular lattice and $A_3Ni_2XO_6$ with $X = \mathrm{Bi}$, Sb, and $A = \mathrm{Li}$, Na on the honeycomb lattice.

The analysis presented in the current work can be extended to a higher spin Kitaev model. For example, Cr^{3+} leaves three electrons in the t_{2g} orbitals that make spin $\frac{3}{2}$ via Hund's coupling assuming that the SOC at Cr sites is negligible compared to Hund's coupling in t_{2g} orbitals, which is likely the case due to a lighter atomic number. Then the superexchange processes via strong spin-orbit coupled anions lead to the Kitaev term, making CrI_3 a candidate for the spin $S = \frac{3}{2}$ Kitaev Mott insulator.

A single layer of CrI_3 shows a ferromagnetic ordering with strong anisotropy [41–43] and investigating the microscopic mechanism of such anisotropy from the bond-dependent interactions is an excellent future study.

A group of van der Waals transition metal halides, such as MX_2 and MX_3, provides a rich family of magnetic materials. The dihalides MX_2 and trihalides MX_3 are made of triangular and honeycomb networks of transition metal cations, respectively, surrounded by edge-shared anions X [44]. When X is heavy, the strong SOC at X sites plays a role in the magnetic mechanism presented in this work. Theoretical studies on these magnetic materials have been limited to the first, second, and third NN Heisenberg model. We propose to revisit these layered $3d$ transitional metal compounds with edge-shared heavy anions from a new perspective of bond-dependent interaction.

There are various experimental ways to test the Kitaev interactions in these candidate materials. Inelastic neutron scattering measurement allows us to map the microscopic spin interactions in these Mott insulators. The magnetic field is a way to induce or reveal the Kitaev spin liquids and its effects have been widely studied in α-$RuCl_3$ [45–60]. Note that the $S = 1$ Kitaev materials suggested here have the antiferromagnetic Kitaev interaction dominant, unlike the $S = \frac{1}{2}$ Kitaev candidate $RuCl_3$ that has the ferromagnetic Kitaev interaction dominant. Thus the magnetic field along the [111] direction may induce the U(1) spin liquid with Fermi surface, similar to the $S = \frac{1}{2}$ case [50,53,54,57–59]. Theoretical studies on $S = 1$ Kitaev materials and experimental studies on a single layer of the proposed materials with and without the magnetic field are interesting projects to pursue in the future. Determining $S = \frac{3}{2}$ Kitaev materials and their magnetic field dependence are also excellent tasks for future studies.

We thank A. Catuneanu for useful discussions during the early stage of the project. This work was supported by the Natural Sciences and Engineering Research Council of Canada, the Center for Quantum Materials at the University of Toronto, and the Canadian Institute for Advanced Research. Computations were performed on the Niagara supercomputer at the SciNet HPC Consortium. SciNet is funded by the Canada Foundation for Innovation under the auspices of Compute Canada; the Government of Ontario; Ontario Research Fund—Research Excellence; and the University of Toronto.

Note added.—Recently, we noted Ref. [61] where a ferromagnetic $S = \frac{3}{2}$ Kitaev interaction is suggested to understand the angle-dependent ferromagnetic resonance experimental data on CrI_3.

*hykee@physics.utoronto.ca

[1] L. Balents, Nature (London) **464**, 199 (2010).
[2] Y. Zhou, K. Kanoda, and T.-K. Ng, Rev. Mod. Phys. **89**, 025003 (2017).
[3] A. Kitaev, Ann. Phys. (Amsterdam) **321**, 2 (2006).
[4] Y. Kasahara, T. Ohnishi, Y. Mizukami, O. Tanaka, S. Ma, K. Sugii, N. Kurita, H. Tanaka, J. Nasu, Y. Motome, T. Shibauchi, and Y. Matsuda, Nature (London) **559**, 227 (2018).
[5] G. Jackeli and G. Khaliullin, Phys. Rev. Lett. **102**, 017205 (2009).
[6] J. Chaloupka, G. Jackeli, and G. Khaliullin, Phys. Rev. Lett. **105**, 027204 (2010).
[7] Y. Singh, S. Manni, J. Reuther, T. Berlijn, R. Thomale, W. Ku, S. Trebst, and P. Gegenwart, Phys. Rev. Lett. **108**, 127203 (2012).
[8] S. K. Choi, R. Coldea, A. N. Kolmogorov, T. Lancaster, I. I. Mazin, S. J. Blundell, P. G. Radaelli, Y. Singh, P. Gegenwart, K. R. Choi, S.-W. Cheong, P. J. Baker, C. Stock, and J. Taylor, Phys. Rev. Lett. **108**, 127204 (2012).
[9] J. Chaloupka, G. Jackeli, and G. Khaliullin, Phys. Rev. Lett. **110**, 097204 (2013).
[10] W. Witczak-Krempa, G. Chen, Y. B. Kim, and L. Balents, Annu. Rev. Condens. Matter Phys. **5**, 57 (2014).
[11] J. G. Rau, Eric Kin-Ho Lee, and H.-Y. Kee, Phys. Rev. Lett. **112**, 077204 (2014).
[12] K. W. Plumb, J. P. Clancy, L. J. Sandilands, V. V. Shankar, Y. F. Hu, K. S. Burch, H.-Y. Kee, and Y.-J. Kim, Phys. Rev. B **90**, 041112(R) (2014).
[13] J. G. Rau and H.-Y. Kee, arXiv:1408.4811.
[14] J. A. Sears, M. Songvilay, K. W. Plumb, J. P. Clancy, Y. Qiu, Y. Zhao, D. Parshall, and Y.-J. Kim, Phys. Rev. B **91**, 144420 (2015).
[15] H.-S. Kim, V. Vijay Shankar, A. Catuneanu, and H.-Y. Kee, Phys. Rev. B **91**, 241110(R) (2015).
[16] L. J. Sandilands, Y. Tian, A. A. Reijnders, H.-S. Kim, K. W. Plumb, Y.-J. Kim, H.-Y. Kee, and K. S. Burch, Phys. Rev. B **93**, 075144 (2016).
[17] L. J. Sandilands, Y. Tian, K. W. Plumb, Y.-J. Kim, and K. S. Burch, Phys. Rev. Lett. **114**, 147201 (2015).
[18] A. Banerjee, C. A. Bridges, J.-Q. Yan, A. A. Aczel, L. Li, M. B. Stone, G. E. Granroth, M. D. Lumsden, Y. Yiu, J. Knolle, S. Bhattacharjee, D. L. Kovrizhin, R. Moessner, D. A. Tennant, D. G. Mandrus, and S. E. Nagler, Nat. Mater. **15**, 733 (2016).
[19] J. G. Rau, E. K.-H. Lee, and H.-Y. Kee, Annu. Rev. Condens. Matter Phys. **7**, 195 (2016).
[20] R. D. Johnson, S. C. Williams, A. A. Haghighirad, J. Singleton, V. Zapf, P. Manuel, I. I. Mazin, Y. Li, H. O. Jeschke, R. Valentí, and R. Coldea, Phys. Rev. B **92**, 235119 (2015).
[21] H.-S. Kim and H.-Y. Kee, Phys. Rev. B **93**, 155143 (2016).
[22] H. B. Cao, A. Banerjee, J.-Q. Yan, C. A. Bridges, M. D. Lumsden, D. G. Mandrus, D. A. Tennant, B. C. Chakoumakos, and S. E. Nagler, Phys. Rev. B **93**, 134423 (2016).
[23] L. Janssen, E. C. Andrade, and M. Vojta, Phys. Rev. B **96**, 064430 (2017).
[24] S. M. Winter, A. A. Tsirlin, M. Daghofer, J. van den Brink, Y. Singh, P. Gegenwart, and R. Valentí, J. Phys. Condens. Matter **29**, 493002 (2017).

[25] G. Baskaran, D. Sen, and R. Shankar, Phys. Rev. B **78**, 115116 (2008).

[26] G. Baskaran, S. Mandal, and R. Shankar, Phys. Rev. Lett. **98**, 247201 (2007).

[27] A. Koga, H. Tomishige, and J. Nasu, J. Phys. Soc. Jpn. **87**, 063703 (2018).

[28] J. Oitmaa, A. Koga, and R. R. P. Singh, Phys. Rev. B **98**, 214404 (2018).

[29] A. M. Samarakoon, A. Banerjee, S.-S. Zhang, Y. Kamiya, S. E. Nagler, D. A. Tennant, S.-H. Lee, and C. D. Batista, Phys. Rev. B **96**, 134408 (2017).

[30] J. Kanamori, Prog. Theor. Phys. **30**, 275 (1963).

[31] P. Fazekas, *Lecture Notes on Electron Correlation and Magnetism* (World Scientific, Singapore, 1999).

[32] See Supplemental Material at http://link.aps.org/supplemental/10.1103/PhysRevLett.123.037203 for hopping matrices $M^{i,j}_{\alpha,\beta}$ of the tight binding model, the energy spectra and exchange paths used in the perturbation method, expressions of spin interactions, and spin-spin correlation obtained from ED.

[33] J. C. Slater and G. F. Koster, Phys. Rev. **94**, 1498 (1954).

[34] Y. Yamaji, Y. Nomura, M. Kurita, R. Arita, and M. Imada, Phys. Rev. Lett. **113**, 107201 (2014).

[35] V. M. Katukuri, S. Nishimoto, V. Yushankhai, A. Stoyanova, H. Kandpal, S. Choi, R. Coldea, I. Rousochatzakis, L. Hozoi, and J. van den Brink, New J. Phys. **16**, 013056 (2014).

[36] R. H. Busey and W. F. Giauque, J. Am. Chem. Soc. **74**, 4443 (1952).

[37] D. Billerey, C. Terrier, N. Ciret, and J. Kleinclauss, Phys. Lett. **61A**, 138 (1977).

[38] S. Kuindersma, J. Sanchez, and C. Haas, Physica (Amsterdam) **111B+C**, 231 (1981).

[39] E. A. Zvereva, M. I. Stratan, Y. A. Ovchenkov, V. B. Nalbandyan, J.-Y. Lin, E. L. Vavilova, M. F. Iakovleva, M. Abdel-Hafiez, A. V. Silhanek, X.-J. Chen, A. Stroppa, S. Picozzi, H. O. Jeschke, R. Valentí, and A. N. Vasiliev, Phys. Rev. B **92**, 144401 (2015).

[40] A. I. Kurbakov, A. N. Korshunov, S. Y. Podchezertsev, A. L. Malyshev, M. A. Evstigneeva, F. Damay, J. Park, C. Koo, R. Klingeler, E. A. Zvereva, and V. B. Nalbandyan, Phys. Rev. B **96**, 024417 (2017).

[41] J. F. Dillon and C. E. Olson, J. Appl. Phys. **36**, 1259 (1965).

[42] M. A. McGuire, H. Dixit, V. R. Cooper, and B. C. Sales, Chem. Mater. **27**, 612 (2015).

[43] B. Huang, G. Clark, E. Navarro-Moratalla, D. R. Klein, R. Cheng, K. L. Seyler, D. Zhong, E. Schmidgall, M. A. McGuire, D. H. Cobden, W. Yao, D. Xiao, P. Jarillo-Herrero, and X. Xu, Nature (London) **546**, 270 (2017).

[44] M. A. McGuire, Crystals **7**, 121 (2017).

[45] R. Yadav, N. A. Bogdanov, V. M. Katukuri, S. Nishimoto, J. Van Den Brink, and L. Hozoi, Sci. Rep. **6**, 37925 (2016).

[46] S.-H. Baek, S.-H. Do, K.-Y. Choi, Y. S. Kwon, A. U. B. Wolter, S. Nishimoto, J. van den Brink, and B. Büchner, Phys. Rev. Lett. **119**, 037201 (2017).

[47] A. U. B. Wolter, L. T. Corredor, L. Janssen, K. Nenkov, S. Schönecker, S.-H. Do, K.-Y. Choi, R. Albrecht, J. Hunger, T. Doert, M. Vojta, and B. Büchner, Phys. Rev. B **96**, 041405(R) (2017).

[48] J. Zheng, K. Ran, T. Li, J. Wang, P. Wang, B. Liu, Z.-X. Liu, B. Normand, J. Wen, and W. Yu, Phys. Rev. Lett. **119**, 227208 (2017).

[49] N. Jansa, A. Zorko, M. Gomilsek, M. Pregelj, K. W. Krämer, D. Biner, A. Biffin, C. Rüegg, and M. Klanjsek, Nat. Phys. **14**, 786 (2018).

[50] Z. Zhu, I. Kimchi, D. N. Sheng, and L. Fu, Phys. Rev. B **97**, 241110(R) (2018).

[51] M. Gohlke, R. Moessner, and F. Pollmann, Phys. Rev. B **98**, 014418 (2018).

[52] J. Nasu, Y. Kato, Y. Kamiya, and Y. Motome, Phys. Rev. B **98**, 060416(R) (2018).

[53] D. C. Ronquillo, A. Vengal, and N. Trivedi, Phys. Rev. B **99**, 140413 (2019).

[54] C. Hickey and S. Trebst, Nat. Commun. **10**, 530 (2019).

[55] S. Liang, M.-H. Jiang, W. Chen, J.-X. Li, and Q.-H. Wang, Phys. Rev. B **98**, 054433 (2018).

[56] P. Lampen-Kelley, L. Janssen, E. C. Andrade, S. Rachel, J. Q. Yan, C. Balz, D. G. Mandrus, S. E. Nagler, and M. Vojta, arXiv:1807.06192.

[57] H.-C. Jiang, C.-Y. Wang, B. Huang, and Y.-M. Lu, arXiv:1809.08247.

[58] L. Zou and Y.-C. He, arXiv:1809.09091.

[59] N. D. Patel and N. Trivedi, Proc. Natl. Acad. Sci. U.S.A. **116**, 12199 (2019).

[60] J. S. Gordon, A. Catuneanu, E. S. Sørensen, and H.-Y. Kee, Nat. Commun. **10**, 2470 (2019).

[61] I. Lee, F. G. Utermohlen, K. Hwang, D. Weber, C. Zhang, J. van Tol, J. E. Goldberger, N. Trivedi, and P. C. Hammel, arXiv:1902.00077.